

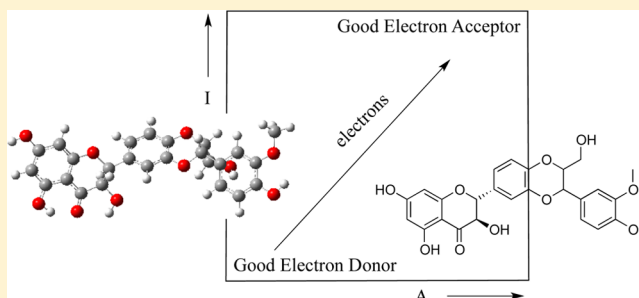
Is Silybin the Best Free Radical Scavenger Compound in Silymarin?

Miguel Reina and Ana Martínez*

Departamento de Materiales de Baja Dimensionalidad Instituto de Investigaciones en Materiales, Universidad Nacional Autónoma de México, Circuito Exterior s/n, CU, P.O. Box 70-360, Coyoacán, 04510 Ciudad de México, México

Supporting Information

ABSTRACT: Silymarin is a natural mixture with beneficial properties for health, specifically due to its antiradical characteristics. The major components of this mixture are silybin (SIL), silychristin (SILYC), isosilybin (ISOSIL), silydianin (SILYD), and taxifolin (TAX). In this report, the electronic properties of these substances are investigated using density functional theory calculations, mainly in order to fully understand the free radical scavenger properties of these compounds. Optimized geometries and Raman spectra are reported. These results could be experimentally useful for identifying some of the major components of the mixture. The relative abundance of deprotonated species under physiological conditions is also included. The free radical scavenger capacity is studied in relation to three mechanisms: the single electron transfer (SET), the radical adduct formation (RAF), and the hydrogen atom transfer (HAT). According to this investigation, the HAT mechanism is the most efficient mechanism for scavenging free radicals for these compounds followed by the RAF mechanism where intramolecular hydrogen bonds are formed in order to stabilize the $\cdot\text{OOH}$ free radical. A particularly important factor is that none of the compounds being studied showed an outstanding antiradical capacity performance compared to the others. In this sense, silymarin is an interesting mixture with antiradical properties and we now know that one single component should be as effective as the mixture.



INTRODUCTION

Milk thistle plant *S. marianum* (L.) Gaertn., Asteraceae¹ was identified previously by the ancient Greeks, but its medicinal properties were first described by the renaissance naturalists. This herbal plant has been consumed for decades because of its beneficial biological properties,^{2–15} which include hepatoprotective,^{3–5} anti-inflammatory,⁶ and anticancer activity.⁸ The active component of the plant, which is extracted from the seeds, is known as silymarin.⁹ Silymarin has been intensively studied in the last decades due to its antioxidant properties and its effectiveness against chemically induced skin damage.^{2–12} It is known that silymarin comprises a very complex mixture of flavonolignans with silybin (SIL) representing the principal and by far the most researched component. Silymarin contains other flavonolignan and flavonoid compounds, named silychristin (SILYC), isosilybin (ISOSIL), silydianin (SILYD), and taxifolin (TAX) (Figure 1). It is interesting to note that SIL, SILYC, ISOSIL, and SILYD are isomers. The mixture also includes other compounds (10–30%) such as 2,3-dehydrosilybin.¹⁴ Furthermore, it was reported that, except for 2,3-dehydrosilybin, none of the major components of silymarin mixture is phototoxic in skin *in vitro* cells.¹⁵

As previously reported, flavonolignans and related compounds are free radical scavengers.^{16–28} The correlation between the structure and the antiradical activity has been demonstrated, in particular for SIL.^{19,28} It has been determined experimentally and theoretically that, for SIL and deprotonated silybin ($\text{SIL}_{(-\text{H})}^{-1}$), principal mechanisms for scavenging free

radicals include the single electron transfer (SET), the hydrogen atom transfer (HAT), and the radical adduct formation (RAF).^{19,28} In spite of studies²⁸ dealing with the antiradical properties of SIL and $\text{SIL}_{(-\text{H})}^{-1}$, there are no reports about the free radical scavenging activity of the other components of silymarin. Silymarin consists of a complex mixture of flavonolignans, which in combination provide strong antiradical properties. Experimental results show excellent antioxidant activity for SIL, that is the major component of silymarin but not necessarily means that it is the best free radical scavenger. In order to reveal which component of the mixture represents the best free radical scavenger, it is important to investigate all of the compounds. To this end, we investigated the antiradical properties of the components of silymarin (SILYC, ISOSIL, SILYD, and TAX). We also provide a comparison with previous SIL results.

As previously reported, the relative abundance of deprotonated species under physiological conditions (pH 7.4) is the key to truly understanding their antioxidant properties.²⁸ Therefore, in this investigation, the relative abundance of deprotonated species at pH 7.4 for each compound is also included, as well as its capacity to stabilize free radicals from the deprotonated species ($\text{SILYC}_{(-\text{H})}^{-1}$, $\text{SIL}_{(-\text{H})}^{-1}$, $\text{ISOSIL}_{(-\text{H})}^{-1}$, $\text{SILYD}_{(-\text{H})}^{-1}$, and $\text{TAX}_{(-\text{H})}^{-1}$). Optimized geometries and

Received: March 17, 2016

Revised: May 4, 2016

Published: May 5, 2016

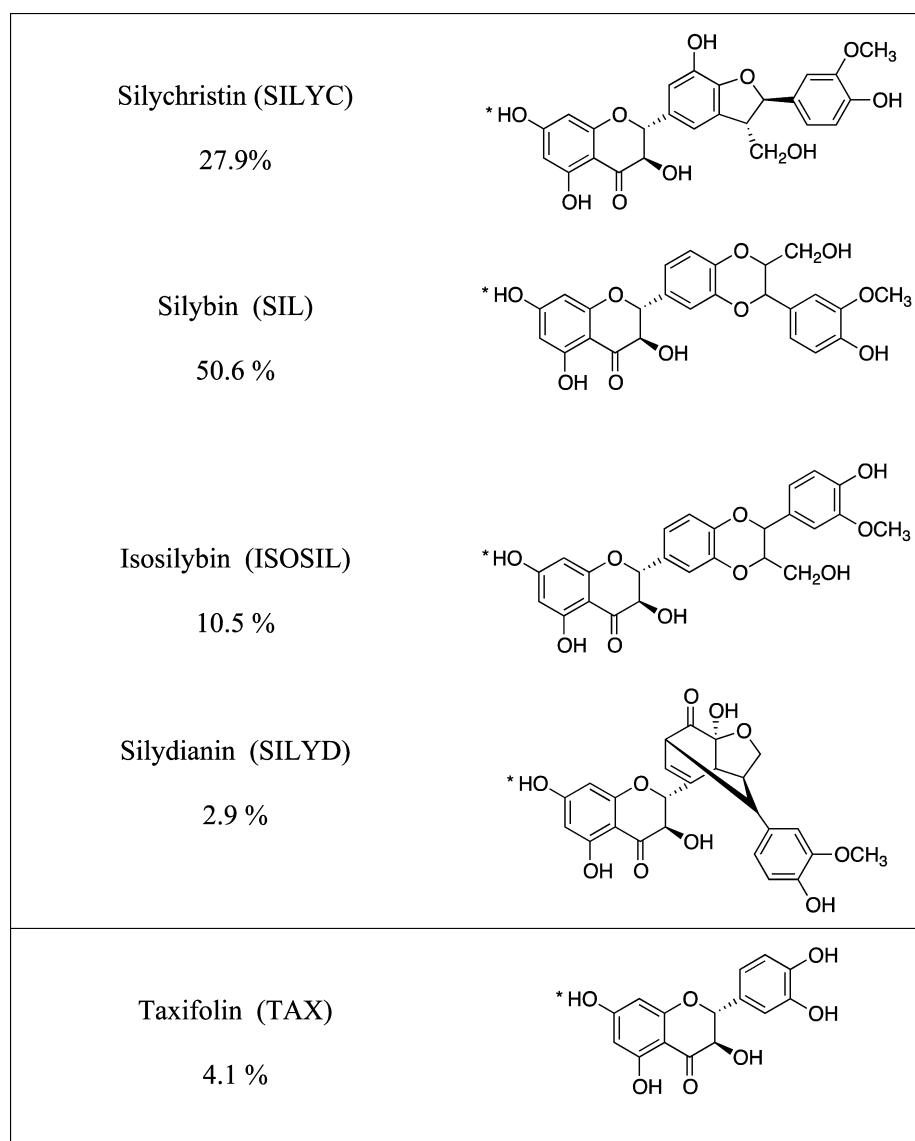


Figure 1. Chemical structures of the major components of silymarin. The labels used in this work are included. Relative abundance (in %) is also reported (Aldrich MDL number MFCD01776359). Stars (*) indicate the acid proton for further reference.

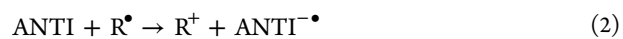
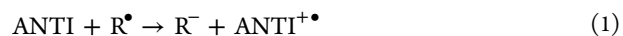
Raman spectra are reported. These results may be experimentally useful for identifying some of the major components of the mixture. The free radical activity is analyzed with regard to three different mechanisms: SET, RAF, and HAT. In the following, it becomes apparent that SIL is neither the most stable isomer nor the best free radical scavenger found in silymarin. In fact, none of the analyzed compounds present outstanding free radical scavenger behavior compared to the others. This is explained by the fact that all molecules share the flavonoid skeleton, which probably guides the antiradical reactivity.

■ COMPUTATIONAL DETAILS

All calculations were carried out with Gaussian 09 implementation.²⁹ Initial geometries were fully optimized at the M06/6-31+G(d) level of theory in the gas phase.^{30–34} This methodology has been successfully used to study small organic molecules.^{28,35–37} Harmonic analyses are calculated to verify local minima (zero imaginary frequencies). Marvin Sketch³⁸ is used to find the pK_a values at 298 K (pK_a min, 0; pK_a max, 14)

and to identify the relative abundance of the deprotonated species under physiological conditions.

The SET mechanism is analyzed using the following schemes:



ANTI represents all the molecules being studied that are reported in Figure 1 and also the corresponding deprotonated compounds. To investigate the SET mechanism, the vertical ionization energy (I) and vertical electron affinity (A) were obtained from single point calculations of the corresponding cationic and anionic molecules, using the optimized structure of the neutrals (or anions for the deprotonated molecules) and the 6-311+G(d,p) basis set. Water and DMSO are included to mimic polar and nonpolar environments. The full electron donor–acceptor map (FEDAM) is a useful, previously defined tool.^{39,40} In this map (Figure 2), I and A are plotted and allow us to classify substances as either donors or acceptors of electrons. Electrons are transferred from molecules located

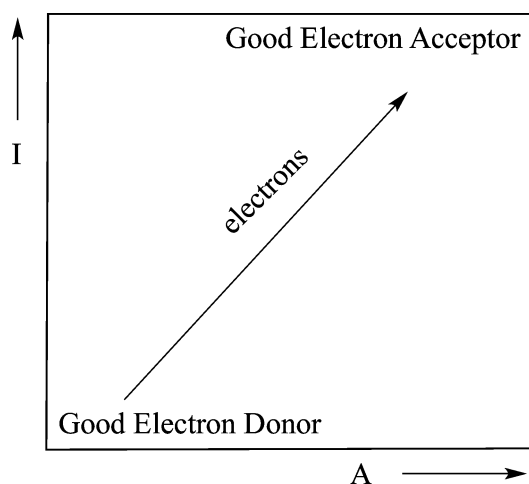
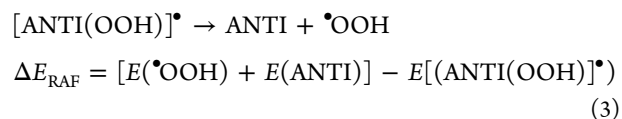


Figure 2. Full electron donor–acceptor map.

down to the left of the map (good electron donors) to those molecules that are up to the right (good electron acceptors).

The RAF mechanism is investigated using $\bullet\text{OOH}$ as a free radical expressed in the following equations.



$\bullet\text{OOH}$ is added to all of the C–C double bonds and also close to a number of oxygen atoms forming hydrogen bonds. The HAT mechanism is analyzed with the hydrogen transfer energy (ΔE_{HAT}) calculated as follows (eq 4)

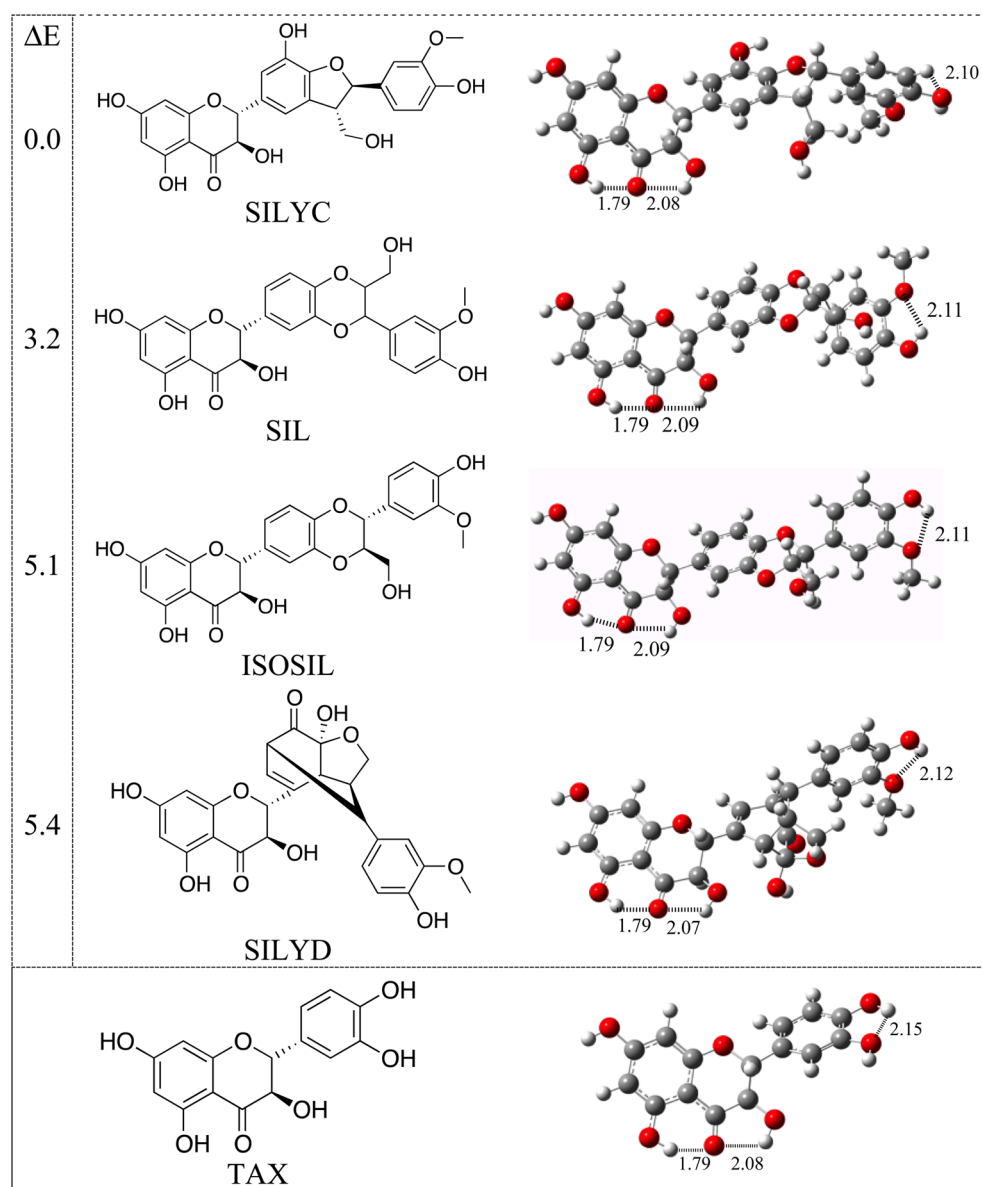
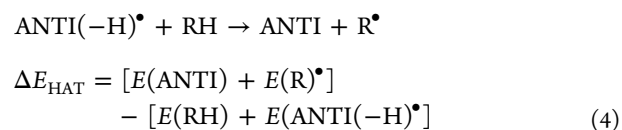


Figure 3. Schematic representation and optimized geometries of major components of silymarin. Molecules inside the dashed square are isomers ($\text{C}_{25}\text{H}_{22}\text{O}_{10}$). ΔE (in kcal/mol) corresponds to the energy differences between the isomers with respect to the most stable.

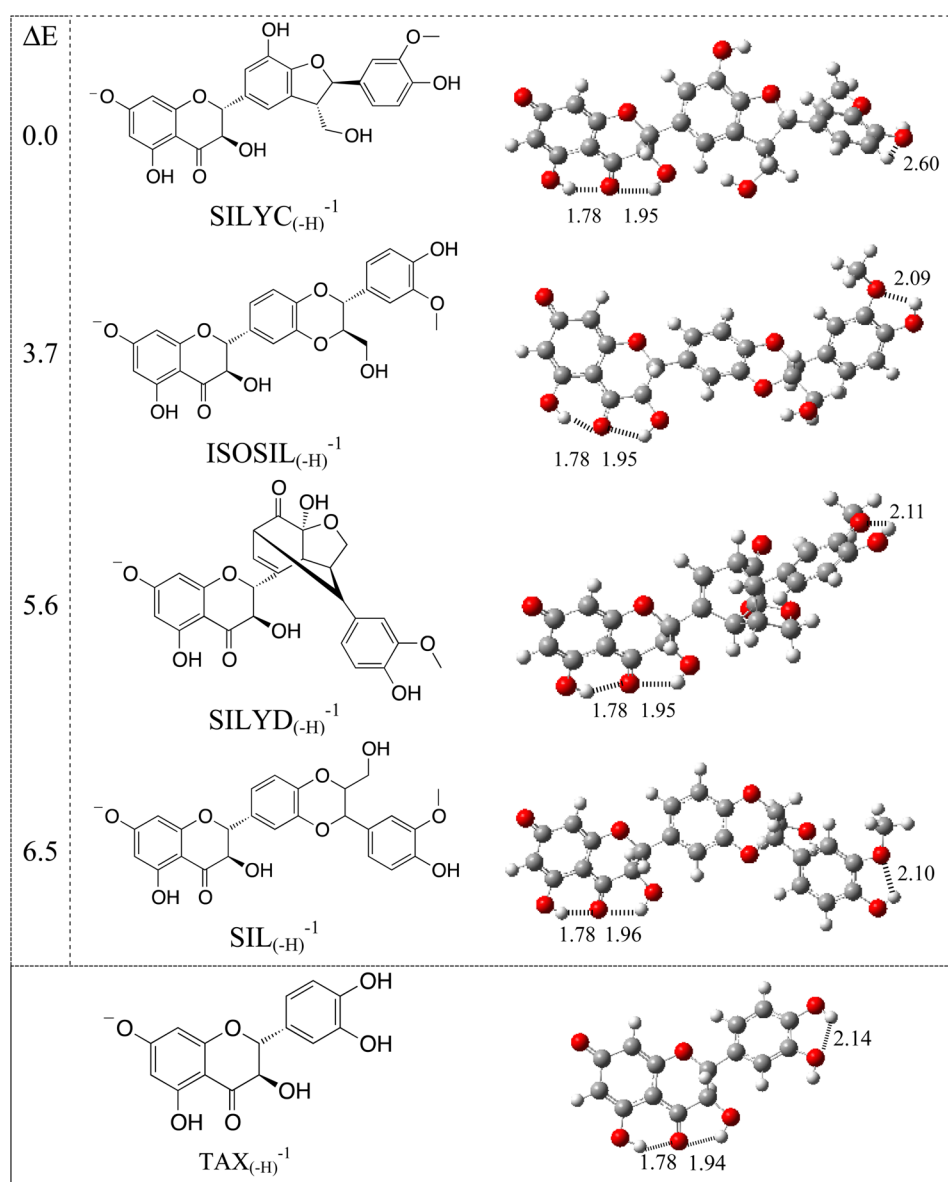


Figure 4. Schematic representation and optimized geometries of major deprotonated components of silymarin. Molecules inside the dashed square are isomers ($C_{25}H_{21}O_{10}$)⁻¹. ΔE (in kcal/mol) corresponds to the energy difference between the isomers with respect to the most stable.

ANTI(-H)[•] is the antiradical molecule, less one hydrogen atom, and RH is the free radical molecule with one bonded H atom. Five different free radicals ($R^{\bullet} = \bullet OH, \bullet OOH, NO_2^{\bullet}, CH_3O^{\bullet},$ and $C_6H_5O^{\bullet}$) are used to analyze this mechanism.

RESULTS AND DISCUSSION

Geometry Optimization. The major components of silymarin may be deprotonated under physiological conditions. The calculated relative abundance at a pH of 7.4 for the five molecules considered in this investigation indicates that 30% are deprotonated (approximately, see Table S1 of the Supporting Information). This result shows it is important to consider the deprotonated compounds in order to complete the description of the antiradical properties under physiological conditions. Previous results for SIL were considered in order to select the initial geometries for optimization.²⁸ It was reported that intramolecular hydrogen bonds are very important for the stabilization of this molecule so that, for this reason, as much as

possible we used initial geometries that contain intramolecular hydrogen bonds.

Figures 3 and 4 present a schematic representation and the optimized structures of SIL, SILYC, ISOSIL, SILYD, and TAX and deprotonated molecules, respectively. In each figure, structures inside the dashed square are isomers, as they have the same chemical formula ($C_{25}H_{22}O_{10}$ and $C_{25}H_{21}O_{10}^{-1}$ for the deprotonated molecules). SILYC is the most stable isomer followed by SIL ($\Delta E = 3.2$ kcal/mol), ISOSIL ($\Delta E = 5.1$ kcal/mol), and SILYD ($\Delta E = 5.4$ kcal/mol). In terms of deprotonated species, SILYC_(-H)⁻¹ is the most stable isomer followed by ISOSIL_(-H)⁻¹ ($\Delta E = 3.7$ kcal/mol), SILYD_(-H)⁻¹ ($\Delta E = 5.6$ kcal/mol), and SIL_(-H)⁻¹ ($\Delta E = 6.5$ kcal/mol). The greatest energy difference is less than 7 kcal/mol, and these compounds can be expected to coexist under experimental conditions.

Figures 3 and 4 present optimized molecules indicating the hydrogen bond lengths (in Å). All optimized structures have at least three hydrogen bonds: two related to the flavonoid

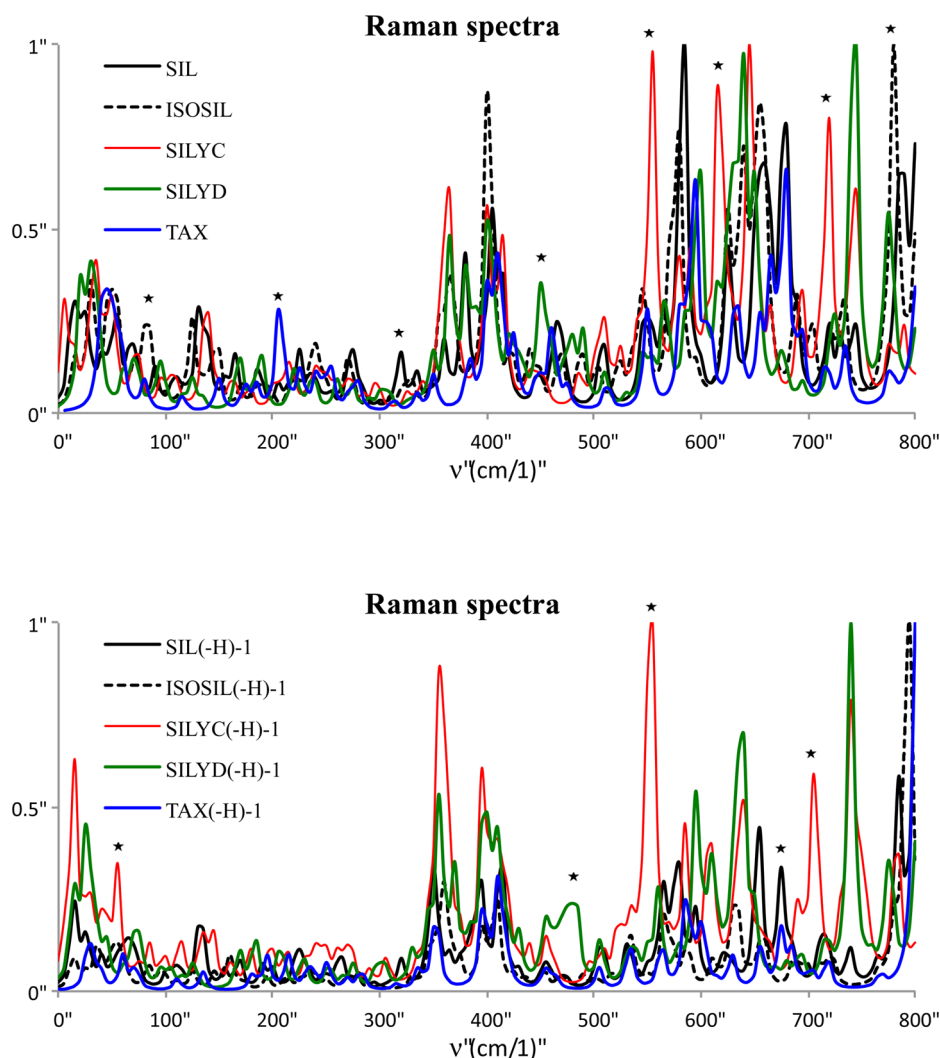


Figure 5. Raman spectra for major components and major deprotonated components of silymarin.

skeleton between the carbonyl and the hydroxyl groups and the third one between OCH_3 and OH of the aromatic ring. TAX also presents intramolecular hydrogen bonds. Comparing the optimized structures, the differences between two of the hydrogen bond lengths are not significant, as they are practically the same, even considering the deprotonated species. However, there is one H bond distance that is shorter for the deprotonated molecules (Figure 4) than for the others (Figure 3). As expected, deprotonated molecules present a stronger H bond.

Raman Spectra. The characterization of these compounds can be made experimentally using infrared and Raman spectra, with the Raman spectra being very useful due to the surface-enhanced-Raman-scattering (SERS) technique. To help with the experimental characterization, Figure 5 reports the theoretical Raman spectra for the compounds under study. There are important differences in the Raman spectra (indicated by stars) that enable us to make the characterization. SIL and ISOSIL are similar, but in the case of ISOSIL, there are two signals at 80 and at 780 cm^{-1} , which are not characteristic of SIL. This difference could be helpful for distinguishing between these two molecules. SILYC presents three signals that are not present for the other compounds at 555, 615, and 720 cm^{-1} , and SILYD shows a unique signal at 450 cm^{-1} . TAX, the

only molecule that is not an isomer, shows an exclusive signal at 205 cm^{-1} . For deprotonated compounds, we also found significant differences. For $\text{SIL}_{(-\text{H})}^{-1}$, a unique signal around 675 cm^{-1} was found. For $\text{SILYC}_{(-\text{H})}^{-1}$, there are three major signals at 55, 555, and 705 cm^{-1} . Finally, for $\text{SILYD}_{(-\text{H})}^{-1}$, there is a signal around 475 cm^{-1} that is not present in the case of the other molecules. For $\text{ISOSIL}_{(-\text{H})}^{-1}$ and $\text{TAX}_{(-\text{H})}^{-1}$, no distinguishable signals were found in the Raman spectra. Comparing the two Raman spectra, we were able to distinguish the deprotonated compounds. SIL presents an important peak at 585 cm^{-1} that is not evident in the case of $\text{SIL}_{(-\text{H})}^{-1}$. Identification of SILYC and $\text{SILYC}_{(-\text{H})}^{-1}$ is possible due to the signal around 15 cm^{-1} for $\text{SILYC}_{(-\text{H})}^{-1}$. ISOSIL shows an important signal at 400 cm^{-1} , which is not present for $\text{ISOSIL}_{(-\text{H})}^{-1}$. For SILYD and $\text{SILYD}_{(-\text{H})}^{-1}$, the shape of the signal around 475 cm^{-1} changes significantly, making it possible to distinguish one from another. Finally, we were able to recognize TAX to $\text{TAX}_{(-\text{H})}^{-1}$ because of the signal at 205 cm^{-1} of TAX. For deprotonated compounds, Raman spectra are less intense. The main conclusion concerning the Raman spectra is that it makes it possible to characterize different components of the mixture and also the deprotonated molecules.

Antiradical Capacity. Single Electron Transfer (SET). The full electron donor–acceptor maps of the molecules being

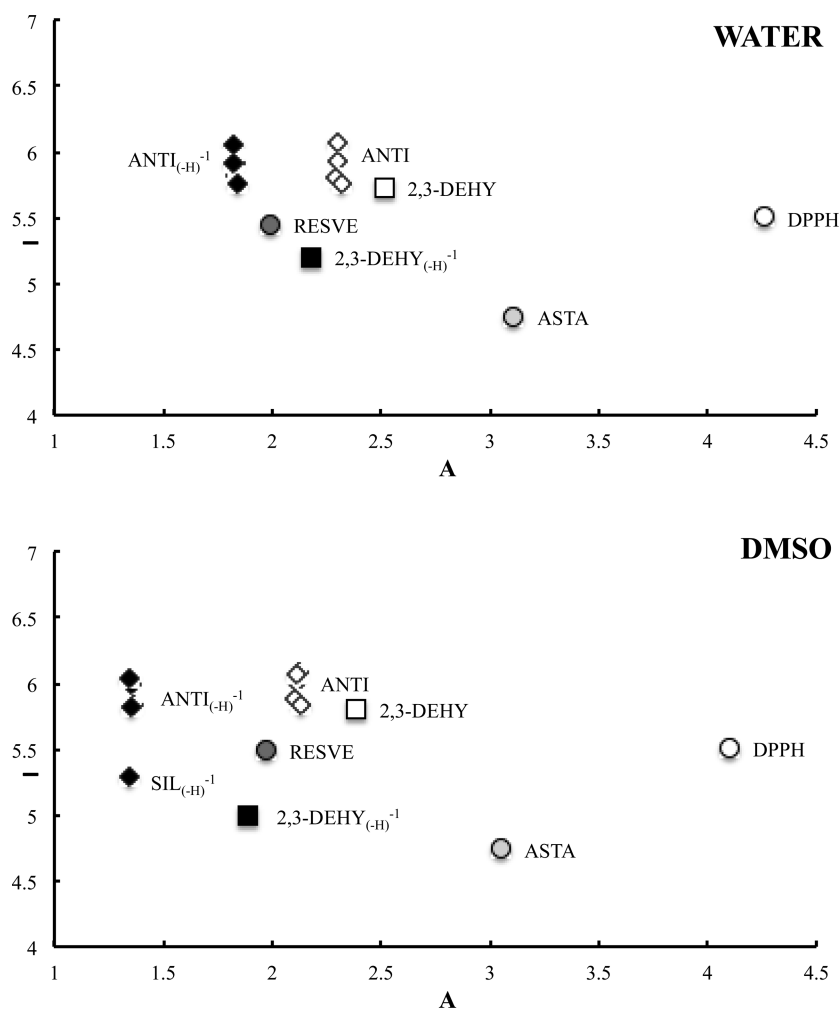


Figure 6. Full electron donor–acceptor map for the major components of silymarin mixture and their deprotonated compounds. DPPH[•], astaxanthin (ASTA), resveratrol (RESVE), 2,3-dehydrosilybin (2,3-DEHY), and deprotonated 2,3-dehydrosilybin (2,3-DEHY_(-H)⁻¹) are included for comparisons.

studied are reported in Figure 6, considering water and DMSO as solvent to mimic polar and nonpolar environment. Astaxanthin (ASTA), resveratrol (RESVE), silybin (SIL), deprotonated silybin (SIL_(-H)⁻¹), 2,3-dehydrosilybin (2,3-DEHY), and deprotonated 2,3-dehydrosilybin (2,3-DEHY_(-H)⁻¹) were reported previously²⁸ and are included for purposes of comparison. DPPH[•] is taken into account, as it is a stable free radical that is very useful for experimental determination of free radical scavenger activity. All compounds in the study present higher *I* values than ASTA, RESVE, and DPPH[•], meaning that none can transfer electrons to DPPH[•]. As electron acceptors, all neutral molecules represent slightly better electron acceptors than RESVE but worse than ASTA and DPPH[•]. As expected, deprotonated molecules represent worse electron acceptors (smaller *A* values) than the others. Except for SIL_(-H)⁻¹ in DMSO which presents a smaller *I* value and represents a better electron donor, the other deprotonated molecules do not represent better electron donors than the neutral molecules. Comparing with 2,3-DEHY and 2,3-DEHY_(-H)⁻¹, it is evident that major components of silymarin represent worse electron donors (*I* larger) and, therefore, worse free radical scavengers than 2,3-DEHY. As previously reported,²⁸ both SIL_(-H)⁻¹ and 2,3-DEHY_(-H)⁻¹ are able to donate electrons to stabilize DPPH[•] with the transfer electron

mechanism being less effective for SIL_(-H)⁻¹. This concurs with previous experimental results indicating that this last molecule represents a better free radical scavenger than SIL.²⁸ The conclusion from the SET mechanism is that no significant differences are apparent among the major components of silymarin mixture. As a result, major silymarin components are not able to either donate or accept electrons from DPPH[•]. Due to its position on the map, none of the major compounds included in the silymarin mixture is able to stabilize DPPH[•] by the electron transfer mechanism. Only SIL_(-H)⁻¹, in a nonpolar environment such as DMSO, could effectively stabilize DPPH[•].

Radical Adduct Formation (RAF). Except for SIL,²⁸ there are no experimental or theoretical results that analyze the free radical scavenging properties of the major compounds of silymarin mixture with [•]OOH. In this report, we analyze the adduct formation mechanism using [•]OOH as a free radical and 10 molecules as free radical scavengers (SILYC, SIL (reported previously),²⁸ ISOSIL, SILYD, TAX, SILYC_(-H)⁻¹, SIL_(-H)⁻¹, ISOSIL_(-H)⁻¹, SILYD_(-H)⁻¹, and TAX_(-H)⁻¹). The [•]OOH radical was systematically added to every C–C, C–O double bond or close to the oxygen atoms where hydrogen bonds can be formed. All systems were fully optimized. Tables S2–S11 show the results of dissociation energies for each free radical adduct compound, indicating the position of the addition.

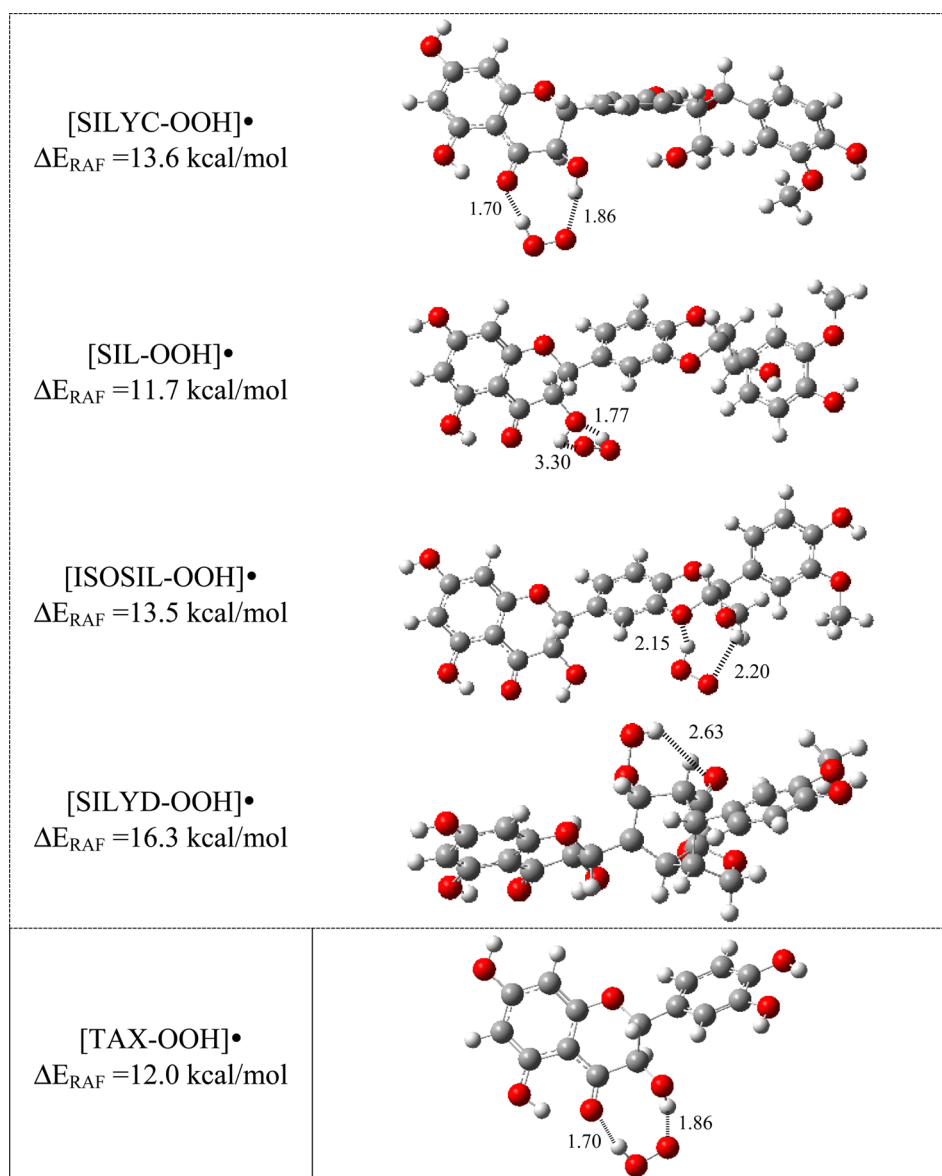


Figure 7. Optimized structures for the most stable ANTI adduct with •OOH and the dissociation energies (kcal/mol) for each compound being studied in the following scheme: [ANTI-OOH]• → ANTI + •OOH. Intramolecular hydrogen bonds are formed, and distance lengths are reported in Å.

Positive dissociation energies indicate that the adduct is more stable than the dissociative products. Figures 7 and 8 report the most stable free radical adduct compounds and the ΔE_{RAF} (in kcal/mol) according to eq 3. All [ANTI-OOH]• are stable by more than 10 kcal/mol with respect to their dissociative products, which implies that the adduct formation is thermodynamically favorable. [SILYD-OOH]• is stable by 16.3 kcal/mol, [SILYC-OOH]• and [ISOSIL-OOH]• are also stable with ΔE_{RAF} equal to 13.6 and 13.5 kcal/mol, respectively, whereas [TAX-OOH]• and [SIL-OOH]• present dissociation energy values of 12.0 and 11.7 kcal/mol, respectively. For all of these molecules, •OOH is bonded to ANTI, mainly forming hydrogen bonds at different positions. In Figure 7, hydrogen bond lengths are also presented. Intramolecular hydrogen bond distances vary from 1.70 Å in [SILYC-OOH]• and [TAX-OOH]• to 3.30 Å for [SIL-OOH]•. In Figure 8, it is possible to see that deprotonated adducts are stable by approximately 17–18 kcal/mol. The

deprotonated adducts are slightly more stable than the corresponding neutral molecules. In every deprotonated molecule, the most reactive atom is the O of the carbonyl group, which forms hydrogen bonds with the •OOH. For these molecules, hydrogen bond length does not vary significantly from one compound to another. The hydrogen bond distance between the O from the C=O and the H from the •OOH free radical is 1.55–1.56 Å for all deprotonated species. The hydrogen bond lengths formed between the O of the •OOH and the H atom of the hydroxyl group of deprotonated molecules vary between 1.89 Å for [SILYD_(-H)⁻¹-OOH]• and 1.96 Å for [SILYC_(-H)⁻¹-OOH]•.

In summary, O atoms of major components of silymarin play a key role in stabilizing the •OOH free radical following the RAF mechanism. As for the SET mechanism, the RAF mechanism does not offer significant differences in antiradical capacity among these compounds. In this way, all compounds

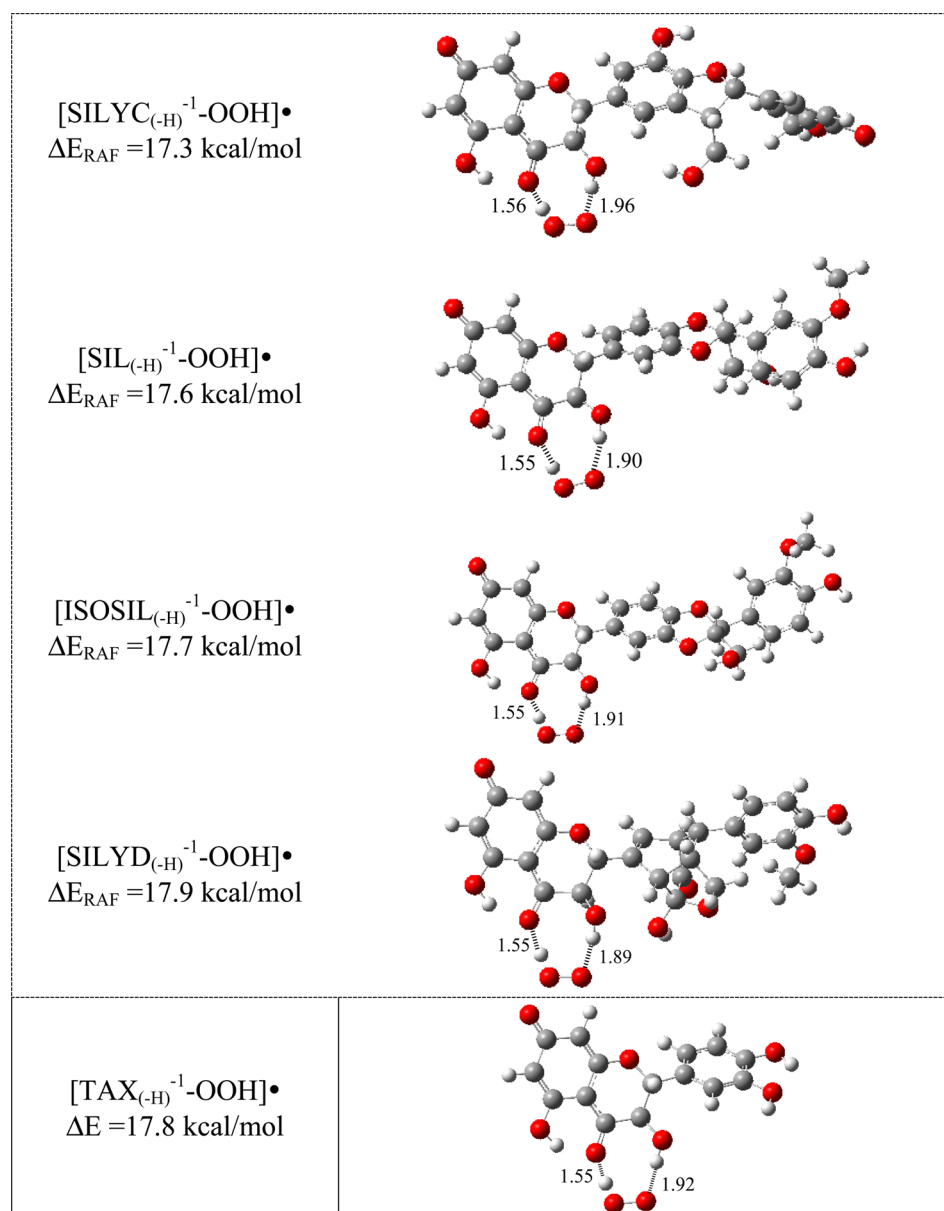


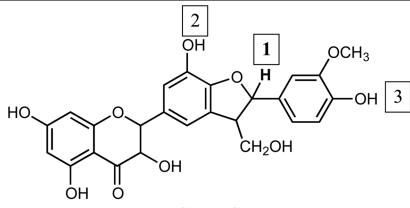
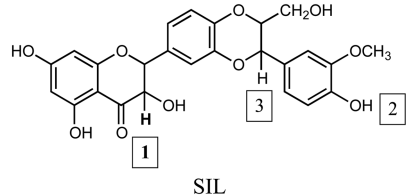
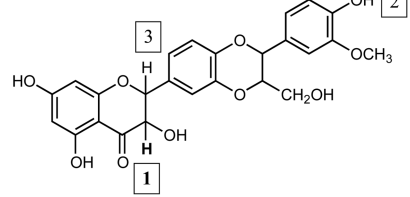
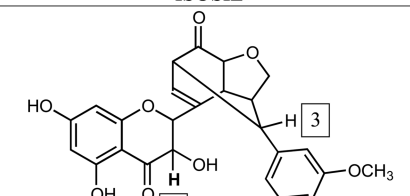
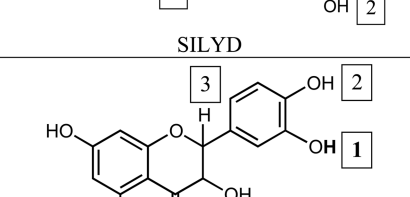
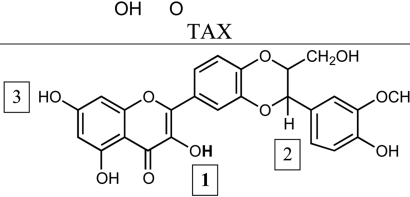
Figure 8. Optimized structures of the most stable ANTI adduct with $\bullet\text{OOH}$ and the dissociation energies (kcal/mol) of each deprotonated compound being studied in the following scheme: $[\text{ANTI}_{(-\text{H})}^{-1}\text{-OOH}]^{\bullet} \rightarrow \text{ANTI}_{(-\text{H})}^{-1} + \bullet\text{OH}$. Intramolecular hydrogen bonds are formed, and distance lengths are reported in Å.

under study show practically the same reactivity for the RAF mechanism with the $\bullet\text{OOH}$ free radical.

Hydrogen Atom Transfer (HAT). In order to evaluate the antiradical capacity of the compounds being studied, we also considered the HAT mechanism. For this purpose, all the hydrogen atoms of the molecules were dissociated one by one, and only the three most stable dehydrogenated molecules were considered for this discussion. The HAT mechanism was analyzed considering five different free radicals: $\bullet\text{OH}$, $\bullet\text{OOH}$, NO_2^{\bullet} , $\text{CH}_3\text{O}^{\bullet}$, and $\text{C}_6\text{H}_5\text{O}^{\bullet}$. Table 1 reports ΔE_{HAT} (see eq 4). Positive ΔE_{HAT} values indicate that the stabilization of the free radical is thermodynamically favorable. According to eq 4 and the selected free radicals, the products RH are H_2O for the $\bullet\text{OH}$ free radical, H_2O_2 for the $\bullet\text{OOH}$ free radical, HNO_2 for the NO_2^{\bullet} free radical, and CH_3OH and $\text{C}_6\text{H}_5\text{OH}$ for $\text{CH}_3\text{O}^{\bullet}$ and $\text{C}_6\text{H}_5\text{O}^{\bullet}$, respectively.

As far as we know, the only HAT study for these molecules was carried out by Trouillas et al.¹⁹ These authors reported the bond dissociation enthalpies of the H atom for four OH groups for SIL and 2,3-DEHY. The abstraction of the H atoms for the remaining positions was not taken into account, and the overall conclusion is that HAT may be the main mechanism for 2,3-DEHY, as it is much more effective for this than for SIL. In this study, we complete this first description by taking into account all H atoms in every molecule being studied and by considering diverse free radicals in the HAT mechanism reaction. As a result of doing this, we found that the H atoms from the hydroxyl group produce stable dehydrogenated molecules, however not necessarily the most stable ones. For SIL, there are two H atoms that do not correspond to OH groups that are reactive (Table 1, SIL, reactive positions 1 and 3). For 2,3-DEHY, there is one reactive position (2, Table 1) that was not considered before. By comparing the reactivity of these

Table 1. HAT Study^a

MOLECULE	Reactive positions	ΔE_{HAT}				
		$\bullet\text{OH}$	$\bullet\text{OOH}$	$\text{NO}_2\bullet$	$\text{CH}_3\text{O}\bullet$	$\text{C}_6\text{H}_5\text{O}\bullet$
 SILYC	1	35.6	3.5	-4.6	21.0	2.3
	2	35.1	3.1	-5.0	20.6	1.9
	3	33.9	1.8	-6.3	19.3	0.6
 SIL	1	36.2	4.1	-4.0	21.7	2.9
	2	32.9	0.8	-7.3	18.3	-0.4
	3	32.6	0.5	-7.6	18.1	-0.7
 ISOSIL	1	36.3	4.3	-3.9	21.8	3.0
	2	33.4	1.3	-6.8	18.8	0.1
	3	29.6	-2.5	-10.6	15.0	-3.7
 SILYD	1	38.9	6.9	-1.3	24.4	5.6
	2	34.1	2.1	-6.0	19.6	0.9
	3	31.5	-0.6	-8.7	16.9	-1.8
 TAX	1	41.8	9.7	1.6	27.3	8.5
	2	33.2	1.2	-7.0	18.7	-0.1
	3	30.9	-1.1	-9.2	16.4	-2.3
 2,3-DEHY	1	34.2	2.1	-6.0	19.6	0.9
	2	32.6	0.5	-7.6	18.0	-0.7
	3	28.3	-3.8	-11.9	13.7	-5.0

^a ΔE_{HAT} values (in kcal/mol) for the indicated H atom are presented.

molecules with different free radicals, we determined that the HAT mechanism is not more important for 2,3-DEHY than for SIL. In this way, this report completed what Trouillas et al. previously initiated.¹⁹

As expected, all analyzed compounds are able to stabilize the $\bullet\text{OH}$ free radical, as this is the most unstable and reactive free radical. All molecules showed three positive and high values of ΔE_{HAT} when the reaction is with this free radical. The stabilization of $\bullet\text{OOH}$ free radical is also possible for all compounds. ΔE_{HAT} are smaller than those for the reaction with $\bullet\text{OH}$, but they are positive and the reaction is feasible. Notably,

according to the HAT mechanism, none of the compounds being studied is able to stabilize $\text{NO}_2\bullet$, as all ΔE_{HAT} values are negative (the exception is a small positive value for TAX). For the $\text{CH}_3\text{O}\bullet$, we observe a similar behavior to that of $\bullet\text{OH}$ because every molecule is capable of stabilizing this free radical and shows high values of ΔE_{HAT} . The greatest difference in terms of the antiradical capacity of these molecules following the HAT mechanism occurs with $\text{C}_6\text{H}_5\text{O}\bullet$. For the dehydrogenated stable molecules studied, the only significant value is for TAX (8.5 kcal/mol) and SILID (5.6 kcal/mol). The

other dehydrogenated compounds present positive values considering one or two positions, but the values are small.

This analysis provides an indication of the free radical capacity of each of the compounds. In spite of this, the main conclusion concerning the HAT mechanism is that none of the compounds shows significantly greater antiradical reactivity compared to the others. This corroborates the proposition that what makes silymarin a strong antiradical mixture is not one component. One single component should be as effective as the mixture.

CONCLUSIONS

The main conclusion of this investigation is that SIL is neither the most stable compound nor the best free radical scavenger considering the major components of silymarin mixture in terms of single electron transfer (SET), radical adduct formation (RAF), and hydrogen atom transfer (HAT) mechanisms. In fact, none of the compounds analyzed manifest better antiradical reactivity than the others. Accordingly, silymarin is an interesting mixture with antiradical properties and now we know that one single component should be as effective as the mixture.

It is possible to identify some of the more abundant components of the mixture applying Raman spectroscopy. Raman spectra allows us to identify four major components and three major deprotonated compounds of the silymarin mixture: SILYC, ISOSIL, SILYD, and TAX and $\text{SILYC}_{(-\text{H})}^{-1}$, $\text{SIL}_{(-\text{H})}^{-1}$, and $\text{SILYD}_{(-\text{H})}^{-1}$.

The SET mechanism shows that deprotonated compounds represent slightly better electron donors but worse electron acceptors than neutral molecules, but in both cases, molecules show similar electron donor–acceptor capacity.

The analysis of the RAF mechanism with $\bullet\text{OOH}$ allows us to conclude that deprotonated species increase the stability of formed adduct but the antiradical capacity is practically the same for every molecule analyzed.

Hydrogen atom transfer (HAT) mechanisms indicated that, from a global point of view, no notable difference exists between any of the molecules.

For the compounds being analyzed, the SET mechanism appears to be the least favorable for stabilizing free radicals, whereas the HAT mechanism is apparently the most propitious. In the case of the RAF mechanism, stable free radical adducts are formed but notably it is possible to make successive additions in order to prove the capacity of this kind of molecule for stabilizing more than one free radical. This offers an interesting subject for further investigation.

ASSOCIATED CONTENT

Supporting Information

The Supporting Information is available free of charge on the ACS Publications website at DOI: 10.1021/acs.jpcc.6b02807.

Optimized structures, relative abundance of compound under study at physiological conditions, and complete references with more than 10 authors (PDF)

AUTHOR INFORMATION

Corresponding Author

*E-mail: martina@unam.mx. Phone: (52-5) 56 22 4500. Web page: <http://www.iim.unam.mx/martina/>.

Notes

The authors declare no competing financial interest.

ACKNOWLEDGMENTS

This study was funded by DGAPA-PAPIIT, Consejo Nacional de Ciencia y Tecnología (CONACyT), and resources provided by the Instituto de Investigaciones en Materiales (IIM). This work was carried out using a NES supercomputer, provided by Dirección General de Cómputo y Tecnologías de Información y Comunicación (DGTIC), Universidad Nacional Autónoma de México (UNAM). We would like to thank the DGTIC of UNAM for their excellent and free supercomputing services and Caroline Karlsake (Masters, Social Anthropology, Cambridge University, England) for reviewing the grammar and style of the text in English. The authors would like to acknowledge Oralia L Jiménez A., María Teresa Vázquez, and Caín González for their technical support. M.R. thanks CONACyT for the PhD scholarship (387687).

REFERENCES

- (1) Morazzoni, P.; Bombardelli, E. *Silybum marianum* (*Carduus marianus*). *Fitoterapia* **1995**, *LXVI*, 3–42.
- (2) Milić, N.; Millosević, N.; Suvajdzic, L.; Zarkov, M.; Abenavoli, L. New therapeutic potentials of milk thistle (*Silybum marianum*). *Nat. Prod. Commun.* **2013**, *8*, 1801–1810.
- (3) Saller, R.; Meier, R.; Brignoli, R. The use of silymarin in the treatment of liver diseases. *Drugs* **2001**, *61*, 2035–2063.
- (4) Wellington, K.; Jarvis, B. Silymarin: A review of its clinical properties in the management of hepatic disorders. *BioDrugs* **2001**, *15*, 465–489.
- (5) Loguercio, C.; Festi, D. Silybin and the liver: from basic research to clinical practice. *World J. Gastroenterol.* **2011**, *17*, 2288–2301.
- (6) Gažák, R.; Walterová, D.; Křen, V. Silybin and silymarin-new and emerging applications in medicine. *Curr. Med. Chem.* **2007**, *14*, 315–338.
- (7) Balian, S.; Ahmad, S.; Zafar, R. Antiinflammatory activity of leaf and leaf callus of *Silybum marianum* (*L.*) Gaertn. in albino rats. *Indian J. Pharmacology* **2006**, *38*, 213–214.
- (8) Agarwal, R.; Agarwal, C.; Ichikawa, H.; Singh, R. P.; Aggarwal, B. H. Anticancer potential of silymarin: from bench to bed side. *Anticancer Res.* **2006**, *26*, 4457–4498.
- (9) Wagner, H.; Hörhammer, L.; Münster, R. On the chemistry of silymarin (silybin), the active principle of the fruits of *Silybum marianum* (*L.*) Gaertn. (*Carduus marianus* *L.*). *Arzneimittelforschung* **1968**, *18*, 688–696.
- (10) Mira, L.; Silva, M.; Manso, C. F. Scavenging of reactive oxygen species by silibinin dihemisuccinate. *Biochem. Pharmacol.* **1994**, *48*, 753–759.
- (11) Gažák, R.; Svobodová, A.; Psotová, J.; Sedmera, P.; Prikrylová, V.; Walterová, D.; Křen, V. Oxidised derivatives of silybin and their antiradical and antioxidant activity. *Bioorg. Med. Chem.* **2004**, *12*, 5677–5687.
- (12) Katiyar, S. K. Silymarin and skin cancer prevention: anti-inflammatory, antioxidant and immunomodulatory effects. *Int. J. Oncol.* **2005**, *26*, 169.
- (13) Šimánek, V.; Křen, V.; Ulrichová, J.; Vicar, J.; Cvak, L. Silymarin: what is in the name...? An appeal for a change of editorial policy. *Hepatology* **2000**, *32*, 442–444.
- (14) Abenavoli, L.; Capasso, R.; Milić, N.; Capasso, F. Milk thistle in liver diseases: past, present, future. *Phytother. Res.* **2010**, *24*, 1423–1432.
- (15) Rajnochová Svobodová, A.; Zálešák, B.; Biedermann, D.; Ulrichová, J.; Vostálová, J. Phototoxic potential of silymarin and its bioactive components. *J. Photochem. Photobiol., B* **2016**, *156*, 61–68.
- (16) Rice-Evans, C. A.; Miller, N. J.; Paganga, G. Antioxidant properties of phenolic compounds. *Trends Plant Sci.* **1997**, *2*, 152–159.
- (17) Martínez, A. Donator acceptor map of psittacofulvins and anthocyanins: are they good antioxidant substances? *J. Phys. Chem. B* **2009**, *113*, 4915–4921.

- (18) Heim, K. E.; Tagliaferro, A. R.; Bobilya, D. J. Flavonoid antioxidants: chemistry, metabolism and structure-activity relationship. *J. Nutr. Biochem.* **2002**, *13*, 572–584.
- (19) Trouillas, P.; Marsal, P.; Svobodová, A.; Vostálová, J.; Gazak, R.; Hrbáč, J.; Sedmera, P.; Kren, V.; Lazzaroni, R.; Duroux, J. L.; et al. Mechanism of the antioxidant action of silybin and 2,3-dehydrosilybin flavonolignans: a joint experimental and theoretical study. *J. Phys. Chem. A* **2008**, *112*, 1054–1063.
- (20) Russo, N.; Toscano, M.; Uccella, N. Semiempirical molecular modeling into quercetin reactive site: structural, conformational, and electronic features. *J. Agric. Food Chem.* **2000**, *48*, 3232–3237.
- (21) Wright, J. S.; Johnson, E. R.; DiLabio, G. A. Predicting the activity of phenolic antioxidants: theoretical methods, analysis of substituent effects and applications to major families of antioxidants. *J. Am. Chem. Soc.* **2001**, *123*, 1173–1183.
- (22) Zhang, H. Y.; Sun, Y. M.; Wang, X. L. Substituents effects on OH bond dissociation enthalpies and ionization potentials of catechols: a DFT study and its implications in that rational design of phenolic antioxidants and elucidation of structure-reactivity relationships for flavonoid antioxidants. *Chem. - Eur. J.* **2003**, *9*, 502–508.
- (23) Leopoldini, M.; Pitarch, I. P.; Russo, N.; Toscano, M. Structure conformation, and electronic properties of apigenin, luteolin, and taxifolin antioxidants. A first principal theoretical study. *J. Phys. Chem. A* **2004**, *108*, 92–96.
- (24) Leopoldini, M.; Marino, T.; Russo, N.; Toscano, M. Density functional computations of the energetic and spectroscopic parameters of quercetin and its radicals in the gas phase and in solvent. *Theor. Chem. Acc.* **2004**, *111*, 210–216.
- (25) György, I.; Antus, S.; Blázovics, A.; Földiák, G. Substituent effects in the free radical reactions of silybin: radiation-induced oxidation of the flavonoid at neutral pH. *Int. J. Radiat. Biol.* **1992**, *61*, 603–609.
- (26) van Wenum, E.; Jurczakowski, R.; Litwinienki, G. Media effects on the mechanism of antioxidant action of silybin and 2,3-dehydrosilybin: role of the enol groups. *J. Org. Chem.* **2013**, *78*, 9102–9112.
- (27) Lemańska, K.; Szymusiak, H.; Tyrakowska, B.; Zieliski, T.; Soffers, A. E. M.; Rietjens, I. M. C. The influence of pH on antioxidant properties and the mechanism of antioxidant action of hydroxylflavones. *Free Radical Biol. Med.* **2001**, *31*, 869–881.
- (28) Reina, M.; Martínez, A. Silybin and 2,3-dehydrosilybin flavonolignans as free radical scavengers. *J. Phys. Chem. B* **2015**, *119*, 11597–11606.
- (29) Frisch, M. J.; Trucks, G. W.; Schlegel, H. B.; Scuseria, G. E.; Robb, M. A.; Cheeseman, J. R.; Scalmani, G.; Barone, V.; Mennucci, B.; Petersson, G. A.; et al. *Gaussian 09*, revision A.08; Gaussian, Inc.: Wallingford, CT, 2009.
- (30) Zhao, Y.; Truhlar, D. G. The M06 suite of density functionals for main group thermochemistry, thermochemical kinetics, non-covalent interactions, excited states, and transition elements: two new functionals and systematic testing of four M06-class functionals and 12 other functionals. *Theor. Chem. Acc.* **2008**, *120*, 215–241.
- (31) Petersson, G. A.; Bennett, A.; Tensfeldt, T. G.; Al-Laham, M. A.; Shirley, W. A.; Mantzaris, J. A complete basis set model chemistry. I. The total energies of closed-shell atoms and hydrides of the first-row atoms. *J. Chem. Phys.* **1988**, *89*, 2193–218.
- (32) Petersson, G. A.; Al-Laham, M. A. A complete basis set model chemistry. II. Open-shell systems and the total energies of the first-row atoms. *J. Chem. Phys.* **1991**, *94*, 6081–6090.
- (33) McLean, A. D.; Chandler, G. S. Contracted Gaussian-basis sets for molecular calculations. 1. 2nd row atoms, $Z = 11-18$. *J. Chem. Phys.* **1980**, *72*, 5639–5648.
- (34) Krishnan, R.; Binkley, J. S.; Seeger, R.; Pople, J. A. Self-Consistent molecular orbital methods. 20. Basis set for correlated wave-functions. *J. Chem. Phys.* **1980**, *72*, 650–54.
- (35) Matisz, G.; Kelterer, A. M.; Fabian, W. M. F.; Kunsági-Máté, S. Coordination of methanol clusters to benzene: a computational study. *J. Phys. Chem. A* **2011**, *115*, 10556–10564.
- (36) Meyer, M. M.; Kass, S. R. Experimental and theoretical gas phase acidities, bond dissociation energies, and heats of formation of HClO_x , $s = 1-4$. *J. Phys. Chem. A* **2010**, *114*, 4086–4092.
- (37) Paukku, Y.; Hill, G. Theoretical determination of one-electron redox potentials for DNA bases, base pairs, and stacks. *J. Phys. Chem. A* **2011**, *115*, 4804–4810.
- (38) Marvin 14.10.27, 2014, ChemAxon (<http://www.chemaxon.com>).
- (39) Martínez, A.; Rodríguez-Gironés, M. A.; Barbosa, A.; Costas, M. Donator acceptor map for carotenoids, melatonin and vitamins. *J. Phys. Chem. A* **2008**, *112*, 9037–9042.
- (40) Martínez, A.; Vargas, R.; Galano, A. What is important to prevent oxidative stress? A theoretical study on electron transfer reactions between carotenoids and free radicals. *J. Phys. Chem. B* **2009**, *113*, 12113–12120.